PSTha5a23, a candidate effector from the obligate biotrophic pathogen *Puccinia striiformis* f. sp. *tritici*, is involved in plant defense suppression and rust pathogenicity

Yulin Cheng[1#], Kuan Wu[2#], Juanni Yao[2], Shumin Li[2], Xiaojie Wang[2], Lili Huang[2], Zhensheng Kang[2]*

[1]State Key Laboratory of Crop Stress Biology for Arid Areas, College of Life Sciences, Northwest A&F University, Yangling 712100, Shaanxi, China

[2]State Key Laboratory of Crop Stress Biology for Arid Areas, College of Plant Protection, Northwest A&F University, Yangling 712100, Shaanxi, China

[#]These authors contributed equally to the work

*To whom correspondence should be addressed: kangzs@nwsuaf.edu.cn

Running title: Characterization of a candidate effector PSTha5a23

This article has been accepted for publication and undergone full peer review but has not been through the copyediting, typesetting, pagination and proofreading process which may lead to differences between this version and the Version of Record. Please cite this article as an 'Accepted Article', doi: 10.1111/1462-2920.13610

Summary

During the infection of host plants, pathogens can deliver virulence-associated "effector" proteins to promote plant susceptibility. However, little is known about effector function in the obligate biotrophic pathogen *Puccinia striiformis* f. sp. *tritici* (*Pst*) that is an important fungal pathogen in wheat production worldwide. Here, we report our findings on an *in planta* highly induced candidate effector from *Pst*, PSTha5a23. The *PSTha5a23* gene is unique to *Pst* and shows a low level of intra-species polymorphism. It has a functional N-terminal signal peptide and is translocated to the host cytoplasm after infection. Overexpression of *PSTha5a23* in *Nicotiana benthamiana* was found to suppress the programmed cell death triggered by BAX, PAMP-INF1, and two resistance-related mitogen-activated protein kinases (MKK1 and NPK1). Overexpression of *PSTha5a23* in wheat also suppressed pattern-triggered immunity (PTI)-associated callose deposition. In addition, silencing of *PSTha5a23* did not change *Pst* virulence phenotypes; however, overexpression of *PSTha5a23* significantly enhanced *Pst* virulence in wheat. These results indicate that the *Pst* candidate effector PSTha5a23 plays an important role in plant defense suppression and rust pathogenicity, and also highlight the utility of gene overexpression in plants as a tool for studying effectors from obligate biotrophic pathogens.

This article has been accepted for publication and undergone full peer review but has not been through the copyediting, typesetting, pagination and proofreading process which may lead to differences between this version and the Version of Record. Please cite this article as an 'Accepted Article', doi: 10.1111/1462-2920.13610

Introduction

As the largest group of plant pathogenic fungi, rust fungi (Uredinales, Basidiomycota) can infect numerous plants in almost all families, including wheat and other grain crops (Aime, 2006). Stripe rust, caused by *Puccinia striiformis* f. sp. *tritici* (*Pst*), is one of the most important diseases affecting wheat production worldwide, particularly in areas that have cool and moist weather conditions during the growing season (Chen et al., 2014). Significant yield losses caused by outbreaks of wheat stripe rust have resulted in economic losses throughout human history (Wellings, 2011). Most resistant wheat varieties used in agricultural production provide only transient protection due to outbreaks of new virulent *Pst* isolates, and stripe rust continues to threaten wheat production and food security on a global scale (Fisher et al., 2012). Thus, an understanding of the molecular basis of *Pst* pathogenesis is of great importance to explore new strategies for durably controlling this disease.

As with other rust fungi, *Pst* is an obligate biotrophic pathogen that must extract nutrients from living plant tissues and cannot grow apart from its hosts. *Pst* can form a specialized infection structure, the haustorium, which makes intimate contact with host cells and permits nutrient uptake (Voegele and Mendgen, 2011). Many putative pathogenicity-related genes were identified in a cDNA library of *Pst* haustoria (Yin et al., 2009). Due to the non-amenability of rust pathosystems (obligate biotrophs infecting host plants) (Petre et al., 2014), *Pst* still lacks an efficient and reliable system for stable transformation, which has long hindered the study of putative pathogenic genes. Recently, host-induced gene silencing (HIGS) has been developed and has proven to be a useful tool to study genes in obligate biotrophic pathogens (Nowara et al., 2010; Yin and Hulbert, 2015). Several *Pst* genes were shown to be important for rust pathogenicity or fungal growth using the barley stripe mosaic virus

(BSMV)-mediated HIGS system (Yin et al., 2011; Zhang et al., 2012; Cheng et al., 2015; Tang et al., 2015; Cheng et al., 2016).

During the infection, pathogens produce an arsenal of effectors that are thought to be major determinants of pathogen virulence in host plants (Jones and Dangl, 2006; Dou and Zhou, 2012). Effectors secreted by pathogens enter host plant cells to suppress plant defense responses and promote plant susceptibility (Giraldo and Valent, 2013). There are two important components of plant immunity, including pattern-triggered immunity (PTI) and effector-triggered immunity (ETI) (Jones and Dangl, 2006). Many characterized effectors from plant pathogens can suppress PTI or/and ETI (de Wit et al., 2009; Guo et al., 2009; Wang et al., 2011). In addition, many plant immune signaling pathways are targeted directly by effectors from distinct pathogen groups (Dou and Zhou, 2012). These studies indicate that pathogen effectors play an important role in the manipulation of host immunity.

Although the role of pathogen effectors is an important topic in the study of plant pathology, less is known about effector function in rust fungi, particularly cereal rust fungi (Duplessis et al., 2011). The haustorium is thought to serve as a structure for delivery of rust effectors into host plant cells (Panstruga and Dodds, 2009), and a few rust effectors have been identified from cDNA libraries constructed from rust haustoria (Hahn and Mendgen, 1997; Catanzariti et al., 2006; Kemen et al., 2013; Yin et al., 2014). In the cDNA library of *Pst* haustoria, Yin et al. (2009) identified 15 genes encoding secreted proteins, six of which were induced during the infection process, and these were considered candidate effectors. In addition, several other candidate effectors from *Pst* were identified with the advancement of *Pst* genome sequencing (Cantu et al., 2011; Zheng et al., 2013). By resequencing the genomes of four *Pst* isolates from the US and the UK, Cantu et al. (2013) identified five *Pst*

This article has been accepted for publication and undergone full peer review but has not been through the copyediting, typesetting, pagination and proofreading process which may lead to differences between this version and the Version of Record. Please cite this article as an 'Accepted Article', doi: 10.1111/1462-2920.13610

candidate effectors that were polymorphic and haustorial expressed secreted proteins. Using heterologous expression screens in *Nicotiana benthamiana*, Petre et al. (2016) also identified a *Pst* candidate effector that associates with processing bodies. However, there is only one report on the role of candidate effectors from *Pst* in manipulating plant immunity and rust pathogenicity (Liu et al., 2016a). Thus, the identification and functional analysis of more candidate effectors from *Pst* will lead to better understanding of effector function in *Pst*.

In this study, we report an *in planta* highly induced candidate effector, PSTha5a23, identified from the cDNA library of *Pst* haustoria (Yin et al., 2009). By silencing *PSTha5a23* using BSMV-mediated HIGS and by overexpressing PSTha5a23 in plants, the specific function of PSTha5a23 was investigated. Our results indicate that PSTha5a23 plays an important role in plant defense suppression and rust pathogenicity, and also highlight the utility of gene overexpression in plants as a tool for studying effectors from obligate biotrophic pathogens.

Results

Features of the candidate effector PSTha5a23

Among the six candidate effectors identified in the cDNA library of *Pst* haustoria (Yin et al., 2009), PSTha5a23 was selected for further study because it had the highest ratio of expression in infected leaves vs. expression in urediniospores or germinated urediniospores. PSTha5a23 is only 108 aa long and lacks any known sequence motifs associated with enzymatic function (Fig. 1A). However, PSTha5a23 contains a putative N-terminal signal peptide (Fig. 1A), which is an important feature of the secretion of effectors (Kale, 2012). To further characterize the specific transcript profiles of *PSTha5a23* in a series of infection stages during the *Pst* life cycle, we assayed its transcriptional abundance by qRT-PCR. The abundance of *PSTha5a23*

was highly induced during the infection of wheat host plants and peaked at two infection stages (Fig. 1B). The first peak, approximately a 8,800-fold increase, occurred at 24 hours post inoculation (hpi), which is the key point for haustoria formation in the parasitic/biotrophic phase. The second peak had an approximate 5,200-fold increase at 216 hpi, which corresponds to the sporulation phase. In addition, we found that *PSTha5a23* was also highly induced (up to 110-fold) during *Pst* sexual reproduction on *Berberis* (Fig. 1B), an alternate host of *Pst* (Jin et al., 2010; Zhao et al., 2013). These results indicate that *PSTha5a23* is highly induced *in planta* and may contribute significantly to plant infection and virulence.

Inter- and intraspecific variation of *PSTha5a23*

Most known pathogen effectors are unique to specific pathogens and exhibit species-specific virulence (Stergiopoulos and de Wit, 2009; Giraldo and Valent, 2013). BLAST analyses revealed that *PSTha5a23* has no homologues in other published genome sequences, indicating that *PSTha5a23* is unique to *Pst*. PSTha5a23 also has no paralogue in *Pst* genome. In addition, sequence alignment showed that the *PSTha5a23* gene has only one nucleotide substitution resulting in an amino acid change among six different *Pst* isolates (Fig. S1). These data indicated that PSTha5a23 is a *Pst*-specific candidate effector with a low level of intra-species polymorphism.

Functional validation of the putative N-terminal signal peptide of PSTha5a23

To confirm the secretory function of the putative N-terminal signal peptide of PSTha5a23 (Fig. 1A), we used a genetic assay based on the requirement of yeast cells for invertase secretion to grow on sucrose or raffinose media (Jacobs et al., 1997; Oh et al., 2009; Tian et al., 2011). The predicted signal peptide sequence of PSTha5a23 was fused in-frame to the mature sequence of yeast invertase in the vector pSUC2

(Jacobs et al., 1997) and was then transformed into the invertase secretion-deficient yeast strain YTK12 (Oh et al., 2009). The empty pSUC2 vector and a non-secreted version of pSUC2 where the signal peptide was substituted with the first part of the Mg87 protein from *Magnaporthe oryzae* (Gu et al., 2011) were used as negative controls, and oomycete effector Avr1b (Shan et al., 2004; Gu et al., 2011) was used as a positive control. The PSTha5a23 construct enabled the invertase mutant yeast strain YTK12 to grow on YPRAA medium (with raffinose instead of sucrose) indicating that the invertase was properly secreted (Fig. 2). This result confirmed that the putative N-terminal signal peptide of PSTha5a23 is a functional secretion signal peptide.

PSTha5a23 is localized to the wheat cytoplasm

After being secreted from pathogens, effectors can enter host plants and target diverse subcellular compartments (Giraldo and Valent, 2013). To determine the subcellular localization of PSTha5a23, a p35S:PSTha5a23-GFP recombinant plasmid was generated and introduced into wheat protoplasts. When the PSTha5a23-GFP fusion protein was transiently expressed in wheat protoplasts, its fluorescence was mainly concentrated in the wheat cytoplasm, while controls expressing only GFP exhibited fluorescence throughout the cell, including the nucleus (Fig. 3). The stability of the PSTha5a23-GFP fusion protein was verified by a western blot (Fig. S2). These results demonstrate that PSTha5a23 is localized to the wheat cytoplasm.

Overexpression of *PSTha5a23* in *N. benthamiana* suppresses programmed cell death

Testing for the ability to suppress mammalian pro-apoptotic factor BAX-triggered programmed cell death (PCD), which physiologically resembles the plant defense-related hypersensitive response (HR) (Lacomme and Cruz, 1999), or *Phytophthora infestans* PAMP (pathogen-associated molecular pattern)

INF1-triggered PCD (Kamoun et al., 1997; Kamoun et al., 1998; Kanzaki et al., 2003), is a valuable assay for effector virulence function (Wang et al., 2011; Giraldo and Valent, 2013). We therefore determined whether overexpression of *PSTha5a23* in the model plant *N. benthamiana* suppresses BAX- or INF1-triggered PCD to investigate the virulence function of candidate effector PSTha5a23. Fig. 4A showed that *A. tumefaciens*-mediated *PSTha5a23* overexpression in *N. benthamiana* could suppress PCD triggered by BAX and INF1, but overexpression of *eGFP* (control) could not suppress the PCD. In addition, proteins MKK1 and NPK1, important components of the mitogen-activated protein kinases (MAPK) cascades of PTI, also triggered PCD in *N. benthamiana* (Cheng et al., 2012). Fig. 4B showed that overexpression of *PSTha5a23* suppressed PCD triggered by MKK1 and NPK1. The accumulations of PSTha5a23 and eGFP proteins in infiltrated tissues were confirmed by a western blotting (Fig. S3A). The accumulations of BAX, INF1, MKK1, and NPK1 proteins in tissues were also validated by a western blotting (Fig. S3B), eliminating the possibility that the suppression of PCD resulted from the breakdown of protein synthesis. These results highlight the virulence function of *PSTha5a23* and suggest that PSTha5a23 plays an important role in suppression of PCD.

Overexpression of *PSTha5a23* in wheat suppresses PTI-associated callose deposition

Recently, a bacterial type III secretion system (T3SS) assay for delivery of fungal effectors into wheat, using the expression/delivery vector pEDV6 and *Pseudomonas fluorescens* effector-to-host analyzer (EtHAn) strain, has been established (Yin and Hulbert, 2011; Upadhyaya et al., 2014). Hence, we overexpressed *PSTha5a23* in wheat cv. Avocet Susceptible (AvS) using this assay to further investigate the role of *PSTha5a23* in plant immunity modulation. *eGFP* and bacterial effector *AvrPto1* that

can trigger HR in wheat (Innes et al., 1993; Yin and Hulbert, 2011) were used as a negative and positive control, respectively. EtHAn is non-pathogenic on wheat (Yin and Hulbert, 2011) and inoculation of EtHAn in wheat could not trigger a detectable necrotic or chlorotic reaction phenotype on wheat plants (Fig. 5A). However, callose deposition was observed on wheat plants inoculated with EtHAn (Fig. 5B), indicating that infection with non-pathogenic EtHAn triggered PTI in wheat. The pEDV6:PSTha5a23, pEDV6:eGFP, and pEDV6:AvrRpt2 constructs were then transferred to the EtHAn strain, which were infiltrated into wheat leaves. The pEDV6:AvrRpt2-inoculated wheat plants exhibited a noticeable HR phenotype in the infiltrated region (Fig. 5A), indicating the expression/delivery system is effective. Both the pEDV6:eGFP- and pEDV6:PSTha5a23-inoculated wheat plants did not show obvious necrosis or chlorosis reaction phenotypes (Fig. 5A), but callose deposition was significantly reduced in the pEDV6:PSTha5a23-inoculated wheat plants compared to the pEDV6:eGFP-inoculated (control) wheat plants (Fig. 5B and C). These results indicate that overexpression of *PSTha5a23* in wheat suppresses PTI-associated callose deposition.

Silencing of *PSTha5a23* does not change *Pst* virulence phenotypes

To investigate the role of *PSTha5a23* in rust pathogenicity, we transiently silenced it using the BSMV-mediated HIGS RNAi system in wheat cv. Suwon 11. Two different fragments (Fig. 6A) were designed for specifically silencing *PSTha5a23*. Ten days after inoculation with BSMV, obvious photo bleaching was observed in the BSMV:TaPDSas-inoculated plants that had the wheat phytoene desaturase (PDS) gene silenced (Fig. S4), indicating that the RNAi system is effective. The BSMV:00- (control), BSMV:PSTha5a23-1as-, and BSMV:PSTha5a23-2as-inoculated wheat plants were then inoculated with virulent *Pst* isolate CYR32, and their rust disease

phenotypes were photographed at 14 days post-inoculation (dpi) with *Pst*. Both BSMV:PSTha5a23-1as- and BSMV:PSTha5a23-2as-inoculated wheat plants showed similar disease phenotypes to the control wheat plants (Fig. 6B), with equivalent amounts of uredinia as the control wheat plants (Fig. 6C). However, qRT-PCR analyses showed that the transcript level of *PSTha5a23* was significantly reduced in the BSMV:PSTha5a23-1as- and BSMV:PSTha5a23-2as-inoculated wheat plants compared to the control wheat plants (Fig. 6D), indicating that *PSTha5a23* was partially knocked down by RNAi. Our results showed that silencing of *PSTha5a23* did not alter *Pst* virulence phenotypes.

Overexpression of *PSTha5a23* enhances rust pathogenicity

We overexpressed *PSTha5a23* in wheat cv. Suwon 11 using bacterial T3SS to further investigate its role in rust pathogenicity. Overexpression of *eGFP* or *PSTha5a23* in Suwon 11 also did not trigger a noticeable necrotic or chlorotic reaction phenotype (Fig. S5). The pEDV6:eGFP- (control) and pEDV6:PSTha5a23-inoculated wheat plants were then inoculated with virulent *Pst* isolate CYR32, and their rust disease phenotypes were photographed at 14 dpi with *Pst*. Fig.7 showed that the rust disease phenotypes in the pEDV6:PSTha5a23-inoculated wheat plants were more severe, with more uredinia formed compared to the control wheat plants. The chlorosis of leaves as an indicator for *Pst* sporulation capacity at early sporulation stage (Ma and Singh, 1996), fungal biomass by qRT-PCR, and fungal growth by microscope in the pEDV6:PSTha5a23-inoculated wheat plants were also greater compared to that in the control wheat plants (Fig. S6-S8), which is consistent with the rust disease phenotype. These results indicate that overexpression of *PSTha5a23* enhanced rust pathogenicity.

Discussion

Effectors play a key role in plant-microbe interactions (Jones and Dangl, 2006), and

many effectors across diverse plant pathogens have been shown to be important virulence factors capable of suppressing plant defense and enhancing pathogenesis (Speth et al., 2007). However, little is known about effector functions in *Pst*. In this study, the function of the *Pst* candidate effector PSTha5a23 was investigated, which provides significant insight into *Pst* pathogenesis.

Overexpression of PSTha5a23 in *N. benthamiana* suppressed PCD triggered by BAX, INF1, MKK1 and NPK1, indicating that PSTha5a23 plays an important role in suppression of PCD. Because the pathogen PAMP INF1 from *P. infestans* and two plant MAPKs (MKK1 and NPK1) are important signaling components of PTI (Kamoun et al., 1997; Jin et al., 2002; Gao et al., 2008), our results suggest that PSTha5a23 is able to suppress PTI-associated PCD. In addition, overexpression of PSTha5a23 in wheat suppressed callose deposition in PTI elicited by the non-pathogenic EtHAn strain, indicating that PSTha5a23 is also able to suppress PTI-associated callose deposition. Previous studies have shown that most effectors from diverse pathogens, including bacteria, oomycete and fungi, can also suppress PTI responses, including callose deposition, inhibition of proteases, generation of reactive oxygen species and PCD (Tao et al., 2003; Thilmony et al., 2006; Truman et al., 2006; van den Burg et al., 2006; Thomas et al., 2009; Fabro et al., 2011; Wang et al., 2011; Liu et al., 2016a). Our results also suggest that the effector PSTha5a23 is functionally located upstream of the PTI signaling, most likely in escaping the recognition by the host plant. These observations highlight the ability of plant pathogens to suppress PTI during the infection of host plants, which is consistent with the conclusion that the PTI signaling pathway is a major battleground that is targeted by many effectors from distinct pathogen groups (Dou and Zhou, 2012).

The abundance of *PSTha5a23* was highly induced during the infection of wheat

host plants, and overexpression of *PSTha5a23* significantly enhanced *Pst* virulence in wheat, indicating that PSTha5a23 contributes significantly to rust pathogenicity. However, silencing *PSTha5a23* did not change *Pst* virulence phenotypes in wheat. Disruption of 77 out of 78 *M. oryzae* candidate effector genes also did not reduce the virulence of *M. oryzae* in rice (Saitoh et al., 2012). In fact, knockdown or knockout of pathogen effectors rarely results in virulence phenotypes, presumably because of functional redundancy (Giraldo and Valent, 2013). In addition, *PSTha5a23* was also found to be upregulated (up to 50-fold) during *Pst* sexual reproduction on *Berberis*, indicating that PSTha5a23 may also contribute to *Pst* infection of alternate host plants. However, three other *Pst* candidate effectors were found to be highly induced during sexual reproduction on *Berberis* but not expressed during asexual reproduction on wheat (Zheng et al., 2013). The infection process of *Pst* on *Berberis* shows some similarity to the infection process in wheat (Zhao et al., 2016). Thus, *Pst* may deliver some common effectors (such as PSTha5a23) to promote plant infection during both asexual and sexual reproductions, or it may deliver some specific effectors to promote plant infection during sexual reproduction.

Obligate biotrophic fungi and Oomycetes, including those causing rust, rusts, powdery mildews and downy mildews, grow only in their plant hosts and lack an efficient and reliable system for stable transformation, which hinders classical genetic studies of their genes, including genes encoding virulence-associated effectors (Voegele and Mendgen, 2011). The function of *Pst* candidate effector PSTha5a23 in this study was mainly revealed by overexpression in plants. Multiple candidate effectors from the obligate biotrophic oomycete pathogen *Hyaloperonospora arabidopsidis* were also shown to suppress plant immunity using T3SS-mediated overexpression in plants (Fabro et al., 2011). These observations highlight the

This article has been accepted for publication and undergone full peer review but has not been through the copyediting, typesetting, pagination and proofreading process which may lead to differences between this version and the Version of Record. Please cite this article as an 'Accepted Article', doi: 10.1111/1462-2920.13610

usefulness of gene overexpression in plants as a tool for studying effectors from obligate biotrophic pathogens.

Future work will be directed toward the investigation of the specific mechanisms by which PSTha5a23 affects plant defense and rust pathogenicity, which could be helpful in planning control strategies of wheat stripe rust.

Experimental Procedures

Plant lines, *Pst* isolate and bacterial strains

Wheat cv. Suwon 11 and AvS, *N. benthamiana*, and Chinese *Pst* isolate CYR32 were used in this study. Wheat plants were grown in a soil mixture in 10 cm diameter pots in a growth chamber under a 16-h photoperiod (60 μmol m^{-2} s^{-1}) at day/night temperatures of 20/16°C and a 60 % relative humidity. *N. benthamiana* plants were grown in a soil mixture in 10 cm diameter pots in a growth chamber under a 12-h photoperiod (60 μmol m^{-2} s^{-1}) at day/night temperatures of 25/22°C and a 60 % relative humidity. Wheat seedlings were inoculated with *Pst* and maintained according to previously described procedures and conditions (Kang et al., 2002).

Escherichia coli JM109 and Top10 were grown in a Luria-Bertani (LB) medium at 37°C and used for plasmid construction. *A. tumefaciens* strain GV3101 was grown in LB medium at 28°C and used for the overexpression of *PSTha5a23* in *N. benthamiana. P. fluorescens* strain EtHAn was grown in a King's B (KB) medium at 28°C and used for overexpression of *PSTha5a23* in wheat plants. Antibiotics were used at final concentrations of 50 μg/ml ampicillin, 50 μg/ml kanamycin, 30 μg/ml rifampicin, 30 μg/ml chloramphenicol, and 25 μg/ml gentamycin.

Plasmid construction

The primers used for plasmid construction in this study are documented in Tables S1.

The Genbank accession number of *PSTha5a23* is GH737046 and mapping to *Pst*

genome in the Broad Institute *Puccinia* database (https://data.broadinstitute.org/annotation/genome/puccinia_group/MultiHome.html) showed that the gene ID of *PSTha5a23* is PSTG_00676. *PSTha5a23* was cloned from the cDNA of *Pst* isolate CYR32 using FastPfu DNA Polymerase (TransGen Biotech, Beijing, China). To validate the secretion function, the predicted signal peptide sequences of PSTha5a23 and Avr1b and the first 25 aa (1-25 aa) of Mg87 (Gu et al., 2011) were fused in-frame to the mature sequence of yeast invertase in the vector pSUC2 (Jacobs et al., 1997). To confirm the subcellular localization of PSTha5a23 in wheat protoplasts, its ORF sequence without the signal peptide was cloned into the pTF486 (designated p35S:GFP) vector (Yu et al., 2008). To silence *PSTha5a23*, a 100-bp fragment containing part of the 5' untranslated region and part of the coding sequence and a 132-bp fragment containing the part of the coding sequence and the 3' untranslated region (Fig. 6A) were cloned into the BSMV gamma vector (Holzberg et al., 2002). The fragments show no similarity with any other *Pst* or wheat gene in BLAST analyses, indicating their specificity. For *PSTha5a23* overexpression in *N. benthamiana* and wheat, its sequence encoding mature protein without the putative signal peptide of *PSTha5a23* was cloned into the PVX vector pGR107 with a Flag-tag fused at the N-terminal (Chen et al., 2015; Jones et al., 1999) and the pEDV6 vector (Sohn et al., 2007). For *eGFP* overexpression in *N. benthamiana* and wheat, its ORF sequence was also cloned into pGR107 with a Flag-tag fused at the N-terminal and pEDV6. Overexpression of *BAX* or *MKK1* in *N. benthamiana* was achieved by cloning their ORF sequences into the PVX vector pGR107 with an HA-tag at the C-terminal (Jones et al., 1999; Chen et al., 2015). Overexpression of *INF1* or *NPK1* in *N. benthamiana* was also achieved by cloning the sequence encoding mature protein without the putative signal peptide of *INF1* and the N terminus only (residues 1 to 373)

of *NPK1* (Wang et al., 2011) into pGR107 with an HA-tag at the C-terminal.

Total RNA extraction and qRT-PCR

The total RNA of urediniospores, germinated urediniospores and infected wheat leaves at 18, 24, 48, 72, 120, 168, and 216 hpi, and infected barberry (*Berberis shensiana*) leaves at 11 dpi were isolated using Trizol™ Reagent (Invitrogen, Carlsbad, USA) following the manufacturer's instructions. After urediniospores were incubated for 10 hours in sterile distilled water in plastic plates at 9℃, germinated urediniospores were then harvested (Zhang et al., 2008). The potential contaminating DNA was digested with DNase I (Promega, Madison, USA) at 37℃ for 30 min and purification with Trizol™ Reagent was repeated to remove DNase I. The quantification of RNA was measured by Nanodrop 2000 (Thermo Scientific, Wilmington, USA) and only RNA samples exhibiting an A260/A280 ratio of 1.8–2.0 and an A260/A230 ratio > 2.0 were used for subsequent analyses. The quality of RNA was evaluated by electrophoresis on ethidium bromide-stained 1.0 % agarose gels and then observed with the Bio-Rad Gel DocTM XR system (Bio-Rad, CA, USA) (Fig. S9). A 2.0-μg RNA aliquot of each sample was used for cDNA synthesis with an oligo$(dT)_{18}$ primer using the Reverse Transcription PCR system (Promega, Madison, USA). Subsequently, the primers for qRT-PCR (Table S1) were designed and qRT-PCR assays were performed using a 7500 Real-Time PCR System (Applied Biosystems, Foster City, USA). The housekeeping gene *Elongation factor 1* (*EF1*) from *Pst*, whose gene ID is PSTG_13111 in the Broad Institute *Puccinia* database, was proven to be the most stable gene and was used as the endogenous reference to normalize gene expression across different *Pst* samples (Yin et al., 2009). The amplicon length of *PSTha5a23* and *PsEF1* is 102 bp and 159 bp, respectively. A single band was obtained on agarose gel electrophoresis from *PSTha5a23* and *PsEF1*

amplifications in several *Pst* infection stages (Fig. S10) and a single peak was also observed in their melting curves (Fig. S11), which proves the specificity of primers. Each PCR mixture contained 0.3 μL 50 × SYBR Green (Invitrogen, Carlsbad, USA), 0.1 μL Rox reference dye (Invitrogen, Carlsbad, USA), 2 μL 10 × cDNA template, 0.4 μL *Taq* DNA polymerase (Thermo Scientific, Wilmington, USA), 2.5 μL 10 × *Taq* buffer (Thermo Scientific, Wilmington, USA), 3.0 μL 25mM $MgCl_2$ (Thermo Scientific, Wilmington, USA), 0.5 μL 10mM dNTP (Thermo Scientific, Wilmington, USA), 0.5 μL of 10 μM forward primer, 0.5 μL of 10 μM reverse primer, and sterile distilled water to a total volume of 25 μL. The following cycling program was used: 95°C for 60 sec, followed by 40 cycles (10 sec at 95°C, 20 sec at 55°C and 40 sec at 72°C). All reactions were performed in triplicate, and reactions without template were used as negative controls. The cDNA of wheat infected with *Pst* was used to prepare standard curves derived from seven serial dilutions and the correlation coefficients for the analysis of the dilution curves were above 0.99 as expected (Fig. S12). Then PCR efficiencies of *PsEF1* and *PSTha5a23* primers were calculated based on their standard curves and the relative gene expression levels were quantified using the Pfaffl analysis method as previously described (Pfaffl, 2001).

Sequence analysis, alignments and polymorphism analysis

The conserved domains of proteins and putative signal peptides were deduced using PFAM (http://pfam.xfam.org/) and SignalP 4.1 (http://www.cbs.dtu.dk/services/ SignalP/), respectively. To check for any homologues of *PSTha5a23* in other organisms, a BLAST analysis was done in NCBI genome sequences. To check for any paralogues of *PSTha5a23* in *Pst* genome, a BLAST analysis was done in the Broad Institute *Puccinia* database.

To identify SNPs in *PSTha5a23*, the *PSTha5a23* coding region from six different

Pst isolates, including one Chinese isolate (CYR32), three US isolates (PST-21, PST-43 and PST-130) and two UK isolates (PST-08-21 and PST-87-7), was analyzed. The genome of CYR32 (Zheng et al., 2013) and the re-sequenced genomes of the three US isolates and two UK isolates (Cantu et al., 2013) were used directly. Sequence data of the six different *Pst* isolate (CYR32, PST-21, PST-43, PST-130, PST-08-21, and PST-87-7) have been deposited in GenBank nucleotide database (http://www.ncbi.nlm.nih.gov/genome/genomes/2580?) under the accession number ANHQ00000000, AORR00000000, AORQ00000000, AEEW00000000, AORS00000000, and AORT00000000, respectively. Local blast searches using BioEdit were conducted to identify the corresponding sequences, and DNAMAN 6.0 was used to create multiple sequence alignments. At each nucleotide position in the alignment, if there were different bases (one or more), one SNP was counted.

Yeast signal sequence trap system

The lithium acetate method (Gietz et al., 1995) was used to transform the pSUC2-derived plasmids into yeast strain YTK12. All transformants were grown on CMD-W medium containing sucrose instead of glucose (0.67% yeast N base without amino acids, 0.075% tryptophan dropout supplement, 2% sucrose, 0.1% glucose, and 2% agar). To assay invertase secretion, positive colonies were cultured on YPRAA plates (1% yeast extract, 2% peptone, 2% raffinose, and 2 mg/mL antimycin A) containing raffinose as the carbohydrate source. The untransformed YTK12 strain and YTK12 strain transformed with an empty pSUC2 vector or the first 25 amino acids of non-secreted Mg87 protein from *M. oryzae* were used as negative controls, while the recombinant YTK12 strain carrying the signal peptide of Avr1b was used as a positive control.

Subcellular localization in wheat protoplasts

The second leaves of wheat seedlings at the two-leaf stage were collected for protoplast transformation. Protoplast isolation, PEG–calcium transfection of plasmid DNA, and protoplast culturing were performed as described previously (Yoo et al., 2007). The GFP signals were then observed using an Olympus BX-53 microscope (Olympus Corporation, Tokyo, Japan) (excitation filter 485 nm, dichromic mirror 510 nm, and barrier filter 520 nm).

A. tumefaciens*-mediated overexpression in *N. benthamiana

The PVX:PSTha5a23 and PVX:eGFP (control) constructs were introduced into the *A. tumefaciens* strain GV3101 by electroporation. For the infiltration of leaves, recombinant strains of *A. tumefaciens* were grown in a LB liquid medium for 48 h, harvested, suspended in an infiltration medium (10 mM $MgCl_2$), and then incubated at room temperature for 1 – 3 h before infiltration. *A. tumefaciens* suspensions were infiltrated at an OD600 of 0.4 into the leaves of 4 – 6-week-old *N. benthamiana* plants using a syringe without a needle.

To assay suppression of BAX/INF1/MKK1/NPK1-induced plant cell death, the PVX:BAX/INF1/MKK1/NPK1 constructs were introduced into *A. tumefaciens*. *A. tumefaciens* cells carrying PSTha5a23 were infiltrated initially, and then *A. tumefaciens* cells carrying BAX/INF1/MKK1/NPK1 were infiltrated into the same site 24 h later. Symptoms were monitored and photographed for 5 dpi with BAX/INF1/MKK1/NPK1. *A. tumefaciens* cells carrying eGFP were infiltrated in parallel as controls.

Western blotting analysis

For verification of protein expression, western blotting was performed as previously described (Liu et al., 2016c). The total proteins in wheat protoplasts or infiltrated tobacco leaves were extracted with protein extraction kits (Solarbio, Beijing, China)

following the manufacturer's instructions. Western blotting assays were performed using the total protein by 12% SDS-PAGE. After proteins were transferred to nitrocellulose membranes (Millipore, Billerica, USA), the membranes were incubated in blocking buffer (0.05% Tween 20 and 5% non-fat milk powder in TBS). Proteins were detected using mouse-derived GFP/HA/Flag-antibodies (Sungene, Tianjing, China) overnight at 4°C. Membranes were washed and incubated with horseradish peroxidase-conjugated anti-mouse secondary antibody (Sungene, Tianjing, China) and chemiluminescence substrate for detection (Sigma, Tokyo, Japan).

Bacterial T3SS-mediated overexpression in wheat plants

The pEDV6:PSTha5a23 construct was transformed into *P. fluorescens* strain EtHAn by electroporation. For the infiltration of leaves, recombinant strains of EtHAn were grown in KB liquid medium for 24 – 48 h, harvested, and suspended in an infiltration medium (10 mM $MgCl_2$). EtHAn suspensions were infiltrated at an OD600 of 0.4 into the second leaves of wheat seedlings at the two-leaf stage using a syringe without a needle. The infiltrated plants were grown and maintained in a cultivation room at 25°C for two days. To check the suppression of callose deposition, pEDV6:PSTha5a23-inoculated wheat (AvS) plants were stained with aniline blue as described previously (Hood and Shew, 1996). To check the involvement in *Pst* pathogenicity, the second leaves in the pEDV6:eGFP- and pEDV6:PSTha5a23-inoculated wheat (Suwon 11) plants were inoculated with fresh *Pst* virulent CYR32 urediniospores. Then, cytological observation of fungal growth and fungal biomass by qRT-PCR were recorded at 72 hpi with *Pst*, chlorosis of wheat leaves were recorded at 216 hpi with *Pst*, and disease symptoms were recorded at 14 dpi with *Pst*.

BSMV-mediated silencing

Capped *in vitro* transcripts were prepared from linearized plasmids containing the tripartite BSMV genome with the mMessage mMachine T7 *in vitro* transcription kit (Ambion, Austin, USA), following the manufacturer's instructions. The second leaf of the wheat (Suwon 11) seedlings at the two-leaf stage was inoculated with BSMV transcripts by gently rubbing the surface with a gloved finger (Holzberg et al., 2002). Three independent sets of plants were prepared for each of the four BSMV constructs (BSMV:00, BSMV:PSTha5a23-1as, BSMV:PSTha5a23-2as, and BSMV:TaPDS). The BSMV-infected plants were maintained in a growth chamber at 25°C. Ten days after BSMV infection, the fourth leaves in the BSMV:00-, BSMV:PSTha5a23-1as- and BSMV:PSTha5a23-2as-inoculated wheat plants were inoculated with fresh virulent CYR32 *Pst* urediniospores. The disease symptoms of the fourth leaves were recorded at 14 dpi with *Pst*. The inoculated fourth leaves were sampled at 24 and 216 hpi with *Pst* for RNA isolation to evaluate the silencing efficiencies of *PSTha5a23* using qRT-PCR as described above.

Uredinial quantification

The *Pst* disease phenotype was quantified by counting the number of uredinia within a 1 cm^2 area at 14 dpi with *Pst*. To avoid bias among the leaf samples, leaves from at least five treated plants were randomly selected. Interpretation of the results was determined by comparing the values of the silenced plants to those of the controls.

Fungal biomass by qRT-PCR

To measure fungal biomass in infected wheat leaves, relative quantification of the single-copy target genes *PsEF1* (from *Pst*) and *TaEF1* (from wheat) by qRT-PCR was carried out as previously described (Panwar et al., 2013; Liu et al., 2016b). Genomic DNA of pEDV6:eGFP- or pEDV6:PSTha5a23-inoculated wheat plants was isolated using the CTAB method as previously described (Zhan et al., 2014). The

quantification and quality of DNA were measured by Nanodrop 2000 (Thermo Scientific, Wilmington, USA) and electrophoresis on ethidium bromide-stained 1.0 % agarose gels, respectively. Subsequently, specific primers were designed as previously described (Liu et al., 2016b) (Table S1) were designed and qRT-PCR assays were performed using a 7500 Real-Time PCR System (Applied Biosystems, Foster City, USA). Total genomic DNA of the wheat cv. Suwon 11 or the *Pst* isolate CYR32 was used to prepare standard curves derived from seven serial dilutions and the correlation coefficients for the analysis of the dilution curves were above 0.99 as expected (Fig. S13). The relative quantities of the PCR products of the *Pst* gene *PsEF1* and the wheat gene *TaEF1* in infected wheat leaves were then calculated using the gene-specific standard curves to quantify the *Pst* and wheat genomic DNA, respectively.

Cytological observation of *Pst* growth

Decolorized wheat specimens were stained with wheat germ agglutinin (WGA) conjugated to Alexa-488 (Invitrogen, Carlsbad, USA) as described previously (Ayliffe et al., 2011), and the stained samples were examined under an Olympus BX-53 fluorescence microscope (Olympus Corporation, Tokyo, Japan) with excitation at 460-480 nm and emission at 495-540 nm.

Acknowledgments

This study was financially supported by the National Natural Science Foundation of China (No. 3143000354), the National Basic Research Program of China (No. 2013CB127700), and the China Postdoctoral Science Foundation (No. 2015M580882).

References

Aime, M.C. (2006) Toward resolving family-level relationships in rust fungi (Uredinales). *Mycoscience* **47:** 112-122.

Ayliffe, M., Devilla, R., Mago, R., White, R., Talbot, M., Pryor, A., and Leung, H. (2011) Nonhost resistance of rice to rust pathogens. *Mol Plant Microbe Interact* **24:** 1143-1155.

Cantu, D., Govindarajulu, M., Kozik, A., Wang, M.N., Chen, X.M., Kojima, K.K. et al. (2011) Next generation sequencing provides rapid access to the genome of *Puccinia striiformis* f. sp. *tritici*, the causal agent of wheat stripe rust. *PLoS One* **6:** e24230.

Cantu, D., Segovia, V., MacLean, D., Bayles, R., Chen, X.M., Kamoun, S. et al. (2013) Genome analyses of the wheat yellow (stripe) rust pathogen *Puccinia striiformis* f. sp. *tritici* reveal polymorphic and haustorial expressed secreted proteins as candidate effectors. *BMC Genomics* **14:** 270.

Catanzariti, A.M., Dodds, P.N., Lawrence, G.J., Ayliffe, M.A., and Ellis, J.G. (2006) Haustorially expressed secreted proteins from flax rust are highly enriched for avirulence elicitors. *Plant Cell* **18:** 243-256.

Chen, C., Liu, S., Liu, Q., Niu, J., Liu, P., Zhao, J., and Jian, H. (2015) An ANNEXIN-like protein from the cereal cyst nematode *Heterodera avenae* suppresses plant defense. *PLoS One* **10:** e0122256.

Chen, W., Wellings, C., Chen, X., Kang, Z., and Liu, T. (2014) Wheat stripe (yellow) rust caused by *Puccinia striiformis* f. sp. *tritici*. *Mol Plant Pathol* **15:** 433-446.

Cheng, B.P., Yu, X.L., Ma, Z.C., Dong, S.M., Dou, D.L., Wang, Y.C., and Zheng, X.B. (2012) *Phytophthora sojae* effector Avh331 suppresses the plant defence response by disturbing the MAPK signalling pathway. *Physiol Mol Plant Pathol* **77:** 1-9.

Cheng, Y., Wang, W., Yao, J., Huang, L., Voegele, R.T., Wang, X., and Kang, Z. (2016) Two distinct Ras genes from *Puccinia striiformis* exhibit differential roles in rust pathogenicity and cell death. *Environ Microbiol*. (http://onlinelibrary.wiley.com/doi/10.1111/1462-2920.13379/full)

Cheng, Y., Wang, X., Yao, J., Voegele, R.T., Zhang, Y., Wang, W. et al. (2015) Characterization of protein kinase PsSRPKL, a novel pathogenicity factor in the wheat stripe rust fungus. *Environ Microbiol* **17:** 2601-2617.

de Wit, P.J.G.M., Mehrabi, R., van den Burg, H.A., and Stergiopoulos, I. (2009) Fungal effector proteins: past, present and future. *Mol Plant Pathol* **10:** 735-747.

Dou, D., and Zhou, J.M. (2012) Phytopathogen effectors subverting host immunity: different foes, similar battleground. *Cell Host Microbe* **12:** 484-495.

Duplessis, S., Joly, D.L., and Dodds, P.N. (2011) 7 Rust effectors. *Effectors in Plant-Microbe Interactions*.

Fabro, G., Steinbrenner, J., Coates, M., Ishaque, N., Baxter, L., Studholme, D.J. et al. (2011) Multiple candidate effectors from the oomycete pathogen *Hyaloperonospora arabidopsidis* suppress host plant Immunity. *PLoS Pathog* **7:** e1002348.

Fisher, M.C., Henk, D.A., Briggs, C.J., Brownstein, J.S., Madoff, L.C., McCraw, S.L. and Gurr, S.J. (2012) Emerging fungal threats to animal, plant and ecosystem health. *Nature* **484:** 186-194.

Gao, M., Liu, J., Bi, D., Zhang, Z., Cheng, F., Chen, S., and Zhang, Y. (2008) MEKK1,

MKK1/MKK2 and MPK4 function together in a mitogen-activated protein kinase cascade to regulate innate immunity in plants. *Cell Res* **18**: 1190-1198.

Gietz, R.D., Schiestl, R.H., Willems, A.R., and Woods, R.A. (1995) Studies on the transformation of intact yeast cells by the LiAc/SS-DNA/PEG procedure. *Yeast* **11**: 355–360.

Giraldo, M.C., and Valent, B. (2013) Filamentous plant pathogen effectors in action. *Nat Rev Microbiol* **11:** 800-814.

Gu, B.A., Kale, S.D., Wang, Q.H., Wang, D.H., Pan, Q.N., Cao, H. et al. (2011) Rust secreted protein Ps87 is conserved in diverse fungal pathogens and contains a RXLR-like motif sufficient for translocation into plant cells. *PLoS One* **6:** e27217.

Guo, M., Tian, F., Wamboldt, Y., and Alfano, J.R. (2009) The majority of the type III effector inventory of *Pseudomonas syringae* pv. tomato DC3000 can suppress plant immunity. *Mol Plant Microbe Interact* **22:** 1069-1080.

Hahn, M., and Mendgen, K. (1997) Characterization of in planta-induced rust genes isolated from a haustorium-specific cDNA library. *Mol Plant Microbe Interact* **10:** 427-437.

Holzberg, S., Brosio, P., Gross, C., and Pogue, G.P. (2002) Barley stripe mosaic virus-induced gene silencing in a monocot plant. *Plant J* **30:** 315-327.

Hood, M., and Shew, H.D. (1996) Applications of KOH-aniline blue fluorescence in the study of plant-fungal interactions. *Phytopathology* **86:** 704-708.

Innes, R.W., Bent, A.F., Kunkel, B.N., Bisgrove, S.R., and Staskawicz, B.J. (1993) Molecular analysis of avirulence gene Avrrpt2 and identification of a putative regulatory sequence common to all known *Pseudomonas syringae* avirulence genes. *J Bacteriol* **175:** 4859-4869.

Jacobs, K.A., Collins-Racie, L.A., Colbert, M., Duckett, M., Golden-Fleet, M., Kelleher, K. et al. (1997) A genetic selection for isolating cDNAs encoding secreted proteins. *Gene* **198:** 289-296.

Jin, H., Axtell, M.J., Dahlbeck, D., Ekwenna, O., Zhang, S., Staskawicz, B., and Baker, B. (2002) NPK1, an MEKK1-like mitogen-activated protein kinase kinase kinase, regulates innate immunity and development in plants. *Dev Cell* **3:** 291-297.

Jin, Y., Szabo, L.J., and Carson, M. (2010) Century-old mystery of *Puccinia striiformis* life history solved with the identification of *Berberis* as an alternate host. *Phytopathology* **100:** 432-435.

Jones, J.D., and Dangl, J.L. (2006) The plant immune system. *Nature* **444:** 323-329.

Jones, L., Hamilton, A.J., Voinnet, O., Thomas, C.L., Maule, A.J., and Baulcombe, D.C. (1999) RNA-DNA interactions and DNA methylation in post-transcriptional gene silencing. *Plant Cell* **11:** 2291-2301.

Kale, S.D. (2012) Oomycete and fungal effector entry, a microbial Trojan horse. *New Phytol* **193:** 874-881.

Kamoun, S., van West, P., Vleeshouwers, V.G.A.A., de Groot, K.E., and Govers, F. (1998) Resistance of *Nicotiana benthamiana* to *Phytophthora infestans* is mediated by the recognition of the elicitor protein INF1. *Plant Cell* **10:** 1413-1425.

Kamoun, S., van West, P., de Jong, A.J., de Groot, K.E., Vleeshouwers, V.G.A.A., and Govers, F. (1997) A gene encoding a host-specific elicitor protein of *Phytophthora infestans* is down-regulated during

infection of potato. *Mol Plant Microbe Interact* **10:** 13-20.

Kang, Z., Huang, L., and Buchenauer, H. (2002) Ultrastructural changes and localization of lignin and callose in compatible and incompatible interactions between wheat and *Puccinia striiformis*. *J Plant Dis Protect* **109:** 25-37.

Kanzaki, H., Saitoh, H., Ito, A., Fujisawa, S., Kamoun, S., Katou, S. et al. (2003) Cytosolic HSP90 and HSP70 are essential components of INF1-mediated hypersensitive response and non-host resistance to *Pseudomonas cichorii* in *Nicotiana benthamiana*. *Mol Plant Pathol* **4:** 383-391.

Kemen, E., Kemen, A., Ehlers, A., Voegele, R., and Mendgen, K. (2013) A novel structural effector from rust fungi is capable of fibril formation. *Plant J* **75:** 767-780.

Lacomme, C., and Cruz, S.S. (1999) Bax-induced cell death in tobacco is similar to the hypersensitive response. *Proc Natl Acad Sci U S A* **96:** 7956-7961.

Liu, C., Pedersen, C., Schultz-Larsen, T., Aguilar, G.B., Madriz-Ordenana, K., Hovmoller, M.S., and Thordal-Christensen, H. (2016a) The stripe rust fungal effector PEC6 suppresses pattern-triggered immunity in a host species-independent manner and interacts with adenosine kinases. *New Phytol*. (http://onlinelibrary.wiley.com/doi/10.1111/nph.14034/full)

Liu, J., Guan, T., Zheng, P., Chen, L., Yang, Y., Huai, B. et al. (2016b) An extracellular Zn-only superoxide dismutase from *Puccinia striiformis* confers enhanced resistance to host-derived oxidative stress. *Environ Microbiol*. (http://onlinelibrary.wiley.com/doi/10.1111/1462-2920.13451/full)

Liu, P., Myo, T.W., Ma, W., Lan, D.Y., Qi, T., Guo, J. et al. (2016c) TaTypA, a ribosome-binding GTPase protein, positively regulates wheat resistance to the stripe rust fungus. *Front Plant Sci* **7:** 873.

Ma, H., and Singh, R.P. (1996) Expression of adult resistance to stripe rust at different growth stages of wheat. *Plant Disease* **80**: 375-379.

Nowara, D., Gay, A., Lacomme, C., Shaw, J., Ridout, C., Douchkov, D. et al. (2010) HIGS: host-induced gene silencing in the obligate biotrophic fungal pathogen *Blumeria graminis*. *Plant Cell* **22:** 3130-3141.

Oh, S.K., Young, C., Lee, M., Oliva, R., Bozkurt, T.O., Cano, L.M. et al. (2009) In planta expression screens of *Phytophthora infestans* RXLR effectors reveal diverse phenotypes, including activation of the *Solanum bulbocastanum* disease resistance protein Rpi-blb2. *Plant Cell* **21:** 2928-2947.

Panwar, V., McCallum, B., and Bakkeren, G. (2013) Endogenous silencing of *Puccinia triticina* pathogenicity genes through in planta-expressed sequences leads to the suppression of rust diseases on wheat. *Plant J* **73:** 521-532.

Panstruga, R., and Dodds, P.N. (2009) Terrific protein traffic: the mystery of effector protein delivery by filamentous plant pathogens. *Science* **324:** 748-750.

Petre, B., Joly, D.L., and Duplessis, S. (2014) Effector proteins of rust fungi. *Front Plant Sci* **5:** 416.

Petre, B., Saunders, D.G.O., Sklenar, J., Lorrain, C., Krasileva, K.V., Win, J. et al. (2016)

Heterologous expression screens in *Nicotiana benthamiana* identify a candidate effector of the wheat yellow rust pathogen that associates with processing bodies. *PLoS One* **11:** e0149035.

Pfaffl, M.W. (2001) A new mathematical model for relative quantification in real-time RT-PCR. *Nucleic Acids Res* **29:** 2003-2007.

Saitoh, H., Fujisawa, S., Mitsuoka, C., Ito, A., Hirabuchi, A., Ikeda, K. et al. (2012) Large-scale gene disruption in *Magnaporthe oryzae* identifies MC69, a secreted protein required for infection by monocot and dicot fungal pathogens. *PLoS Pathog* **8:** e1002711.

Shan, W.X., Cao, M., Dan, L.U., and Tyler, B.M. (2004) The Avr1b locus of *Phytophthora sojae* encodes an elicitor and a regulator required for avirulence on soybean plants carrying resistance gene Rps1b. *Mol Plant Microbe Interact* **17:** 394-403.

Sohn, K.H., Lei, R., Nemri, A., and Jones, J.D. (2007) The downy mildew effector proteins ATR1 and ATR13 promote disease susceptibility in *Arabidopsis thaliana*. *Plant Cell* **19:** 4077-4090.

Speth, E.B., Lee, Y.N., and He, S.Y. (2007) Pathogen virulence factors as molecular probes of basic plant cellular functions. *Curr Opin Plant Biol* **10:** 580-586.

Stergiopoulos, I., and de Wit, P.J.G.M. (2009) Fungal effector proteins. *Annu Rev Phytopathol* **47:** 233-263.

Tang, C., Wei, J., Han, Q., Liu, R., Duan, X., Fu, Y. et al. (2015) PsANT, the adenine nucleotide translocase of *Puccinia striiformis*, promotes cell death and fungal growth. *Sci Rep* **5:** 11241.

Tao, Y., Xie, Z., Chen, W., Glazebrook, J., Chang, H.-S., Han, B. et al. (2003) Quantitative nature of *Arabidopsis* responses during compatible and incompatible interactions with the bacterial pathogen *Pseudomonas syringae*. *Plant Cell* **15:** 317-330.

Thilmony, R., Underwood, W., and He, S.Y. (2006) Genome-wide transcriptional analysis of the *Arabidopsis thaliana* interaction with the plant pathogen *Pseudomonas syringae* pv. tomato DC3000 and the human pathogen *Escherichia coli* O157: H7. *Plant J* **46:** 34-53.

Thomas, W.J., Thireault, C.A., Kimbrel, J.A., and Chang, J.H. (2009) Recombineering and stable integration of the *Pseudomonas syringae* pv. *syringae* 61 hrp/hrc cluster into the genome of the soil bacterium *Pseudomonas fluorescens* Pf0-1. *Plant J* **60:** 919-928.

Tian, M., Win, J., Savory, E., Burkhardt, A., Held, M., Brandizzi, F., and Day, B. (2011) 454 genome sequencing of *Pseudoperonospora cubensis* reveals effector proteins with a QXLR translocation motif. *Mol Plant Microbe Interact* **24:** 543-553.

Truman, W., Zabala, M.T., and Grant, M. (2006) Type III effectors orchestrate a complex interplay between transcriptional networks to modify basal defence responses during pathogenesis and resistance. *Plant J* **46:** 14-33.

Upadhyaya, N.M., Mago, R., Staskawicz, B.J., Ayliffe, M.A., Ellis, J.G., and Dodds, P.N. (2014) A bacterial type III secretion assay for delivery of fungal effector proteins into wheat. *Mol Plant Microbe Interact* **27:** 255-264.

van den Burg, H.A., Harrison, S.J., Joosten, M.H., Vervoort, J., and de Wit, P.J. (2006) *Cladosporium fulvum* Avr4 protects fungal cell walls against hydrolysis by plant chitinases accompanying type-setting, pagination and proofreading process which may lead to differences between this version and the Version of Record. Please cite this article as an 'Accepted Article', doi: 10.1111/1462-2920.13610

Voegele, R.T., and Mendgen, K.W. (2011) Nutrient uptake in rust fungi: how sweet is parasitic

life? *Euphytica* **179:** 41-55.

Wang, Q.Q., Han, C.Z., Ferreira, A.O., Yu, X.L., Ye, W.W., Tripathy, S. et al. (2011) Transcriptional programming and functional interactions within the *Phytophthora sojae* RXLR effector repertoire. *Plant Cell* **23:** 2064-2086.

Wellings, C.R. (2011) Global status of stripe rust: a review of historical and current threats. *Euphytica* **179:** 129-141.

Yin, C., and Hulbert, S. (2011) Prospects for functional analysis of effectors from cereal rust fungi. *Euphytica* **179:** 57-67.

Yin, C., and Hulbert, S. (2015) Host induced gene silencing (HIGS), a promising strategy for developing disease resistant crops. *Gene Technology* **2015**.

Yin, C., Jurgenson, J.E., and Hulbert, S.H. (2011) Development of a host-induced RNAi system in the wheat stripe rust fungus *Puccinia striiformis* f. sp. *tritici*. *Mol Plant Microbe Interact* **24:** 554-561.

Yin, C., Park, J.J., Gang, D.R., and Hulbert, S.H. (2014) Characterization of a tryptophan 2-monooxygenase gene from *Puccinia graminis* f. sp. *tritici* involved in auxin biosynthesis and rust pathogenicity. *Mol Plant Microbe Interact* **27:** 227-235.

Yin, C., Chen, X., Wang, X., Han, Q., Kang, Z., and Hulbert, S. (2009) Generation and analysis of expression sequence tags from haustoria of the wheat stripe rust fungus *Puccinia striiformis* f. sp. *tritici*. *BMC Genomics* **10:** 626.

Yoo, S.-D., Cho, Y.-H., and Sheen, J. (2007) *Arabidopsis* mesophyll protoplasts: a versatile cell system for transient gene expression analysis. *Nat Protoc* **2:** 1565-1572.

Yu, F., Liu, X., Alsheikh, M., Park, S., and Rodermel, S. (2008) Mutations in SUPPRESSOR OF VARIEGATION1, a factor required for normal chloroplast translation, suppress var2-mediated leaf variegation in *Arabidopsis*. *Plant Cell* **20:** 1786-1804.

Zhan, G., Tian, Y., Wang, F., Chen, X., Guo, J., Jiao, M. et al. (2014) A novel fungal hyperparasite of *Puccinia striiformis* f. sp. *tritici*, the causal agent of wheat stripe rust. *PLoS One* **9:** e111484.

Zhang, H., Guo, J., Voegele, R.T., Zhang, J., Duan, Y., Luo, H., and Kang, Z. (2012) Functional characterization of calcineurin homologs PsCNA1/PsCNB1 in *Puccinia striiformis* f. sp. *tritici* using a host-induced RNAi system. *PLoS One* **7:** e49262.

Zhang, Y., Qu, Z., Zheng, W., Liu, B., Wang, X., Xue, X. et al. (2008) Stage-specific gene expression during urediniospore germination in *Puccinia striiformis* f. sp. *tritici*. *BMC Genomics* **9:** 203.

Zhao, J., Wang, L., Wang, Z., Chen, X., Zhang, H., Yao, J. et al. (2013) Identification of eighteen berberis species as alternate hosts of *Puccinia striiformis* f. sp. *tritici* and virulence variation in the pathogen isolates from natural infection of barberry plants in China. *Phytopathology* **103:** 927-934.

Zhao, J., Wang, M., Chen, X., Ma, J., and Kang, Z. S. (2016) Role of alternate hosts in epidemiology and pathogen variation of cereal rusts. *Annu Rev Phytopathol* **54:** 207-228.

Zheng, W.M., Huang, L.L., Huang, J.Q., Wang, X.J., Chen, X.M., Zhao, J. et al. (2013) High

genome heterozygosity and endemic genetic recombination in the wheat stripe rust fungus. *Nat Commun* **4:** 2673.

This article has been accepted for publication and undergone full peer review but has not been through the copyediting, typesetting, pagination and proofreading process which may lead to differences between this version and the Version of Record. Please cite this article as an 'Accepted Article', doi: 10.1111/1462-2920.13610

Figure legends

Fig. 1. The candidate effector PSTha5a23 is highly induced *in planta*. (A) Features of the primary structures of PSTha5a23. SP, signal peptide. (B) Transcription profiles of *PSTha5a23* at different *Puccinia striiformis* f. sp. *tritici* (*Pst*) infection stages determined by qRT-PCR. *Pst* development in wheat can be divided into three major stages: penetration stage (gray), parasitic/biotrophic stage (yellow), and sporulation stage (red). Sexual reproduction on the alternate host *Berberis* is marked in blue. U, urediniospores; GU, germinated urediniospores; 18 h – 216 h, wheat leaves infected with *Pst* at 18 – 216 hpi; B, barberry (*Berberis* spp.) leaves infected with *Pst* at 11 dpi. Relative transcript levels were calculated using the Pfaffl analysis method, and values are expressed relative to an endogenous *Pst* reference gene *EF1*. The results represent the means ± standard errors of three biological replicates. Asterisks indicate a significant difference ($P < 0.05$) relative to the urediniospore sample determined using Student's t-test.

Fig. 2. Functional validation of the putative N-terminal signal peptide of PSTha5a23 using the yeast invertase secretion assay. The sequence of the putative PSTha5a23 signal peptide (Fig. 1 A) was fused in-frame to the invertase sequence in the pSUC2 vector and then transformed into yeast strain YTK12. The untransformed YTK12 strain, empty pSUC2 vector, and the first 25 aa of non-secreted Mg87 protein from *Magnaporthe oryzae* were used as negative controls, and the oomycete effector Avr1b was used as a positive control. Only the yeast strains that are able to secrete invertase can grow on both CMD-W and YPRAA media.

Fig. 3. Subcellular localization of PSTha5a23 in wheat protoplasts. GFP and PSTha5a23-GFP fusion proteins were expressed in wheat protoplasts following PEG-mediated transformation. Nucleus. Bar = 20 μm.

Fig. 4. Overexpression of PSTha5a23 in *Nicotiana benthamiana* suppressed programmed cell death triggered by BAX, PAMP-INF1 (A), and two resistance-related MAPKs (MKK1 and NPK1) (B). *N. benthamiana* leaves were infiltrated with *Agrobacterium tumefaciens* cells containing PVX carrying PSTha5a23 or a control gene (eGFP), either alone or followed after 24 h by *A. tumefaciens* cells carrying PVX:BAX/INF1/MKK1/NPK1.

Fig. 5. Overexpression of PSTha5a23 in wheat (AvS) suppressed PTI-associated callose deposition. (A) The phenotype of wheat leaves inoculated with $MgCl_2$ buffer, EtHAn, pEDV6:eGFP, pEDV6:PSTha5a23, and pEDV6:AvrRpt2 at 72 hpi. (B) The wheat leaves inoculated with $MgCl_2$ buffer, EtHAn, pEDV6:eGFP, or pEDV6:PSTha5a23 were examined for callose deposition by epifluorescence microscopy after aniline blue staining. Bars = 100 μm. (C) Average number of callose deposits/mm^2 in wheat leaves inoculated with $MgCl_2$ buffer, EtHAn, pEDV6:eGFP, or pEDV6:PSTha5a23. Values represent the means ± standard error of three independent samples. Asterisks indicate a significant difference ($P < 0.05$) relative to the pEDV6:eGFP sample according to Student's t-test.

Fig. 6. Functional assessment of *PSTha5a23* in *Puccinia striiformis* f. sp. *tritici* (*Pst*) pathogenicity determined by BSMV-mediated HIGS. (A) Two specific sequence regions for HIGS of *PSTha5a23*. (B) Phenotypes of the fourth leaves of BSMV:00- (control), BSMV:PSTha5a23-1as-, and BSMV:PSTha5a23-2as-inoculated wheat plants 14 dpi with *Pst*. (C) Quantification of the uredinial density in the BSMV:00-, BSMV:PSTha5a23-1as-, and BSMV:PSTha5a23-2as-inoculated wheat plants 14 dpi with *Pst*. Values represent the means ± standard error of three independent assays. (D) Relative transcript levels of *PSTha5a23* in the BSMV:00-, BSMV:PSTha5a23-1as-, and BSMV:PSTha5a23-2as-inoculated wheat plants 24 and 216 hpi with *Pst*. Values

are expressed relative to the endogenous *Pst* reference gene *EF1*, with the empty vector (BSMV:00) set at 1. Values represent the means ± standard error of three independent samples. Differences were assessed using Student's t-tests, and asterisks indicate $P < 0.05$.

Fig. 7. Functional assessment of *PSTha5a23* in *Puccinia striiformis* f. sp. *tritici* (*Pst*) pathogenicity determined by T3SS-mediated overexpression in wheat (Suwon 11). (A) Disease phenotypes of pEDV6:eGFP- (control) and pEDV6:PSTha5a23-inoculated wheat plants 14 dpi with *Pst*. (B) Quantification of uredinial density in pEDV6:eGFP- and pEDV6:PSTha5a23-inoculated wheat plants 14 dpi with *Pst*. Values represent the means ± standard error of three independent assays. Differences were assessed using Student's t-tests, and asterisks indicate $P < 0.05$.

This article has been accepted for publication and undergone full peer review but has not been through the copyediting, typesetting, pagination and proofreading process which may lead to differences between this version and the Version of Record. Please cite this article as an 'Accepted Article', doi: 10.1111/1462-2920.13610

Supporting Information

Fig. S1. Sequence alignment of *PSTha5a23* among different *Puccinia striiformis* f. sp. *tritici* (*Pst*) isolates at the nucleotide (A) and amino acid levels (B). PSTha5a23 only had one nucleotide substitution among six different *Pst* isolates, including one Chinese isolate (CYR32), three US isolates (PST-21, PST-43, and PST-130) and two UK isolates (PST-08/21 and PST-87/7).

Fig. S2. Western blot analysis of the expression of GFP and PSTha5a23-GFP proteins in wheat protoplasts with a GFP-antibody.

Fig. S3. Western blot analysis of protein expressions in *Nicotiana benthamiana*. (A) eGFP and PSTha5a23 were detected with an Flag-antibody. (B) BAX, INF1, MKK1 and NPK1 were detected with an HA-antibody.

Fig. S4. Phenotypes of the fourth leaves of wheat plants 10 dpi with FES buffer (mock) or BSMV:TaPDS.

Fig. S5. The phenotype of wheat (Suwon 11) leaves inoculated with $MgCl_2$ buffer, pEDV6:eGFP, pEDV6:PSTha5a23, and pEDV6:AvrRpt2 at 72 hpi.

Fig. S6. Macroscopic observation of pEDV6:eGFP- (control) and pEDV6:PSTha5a23-inoculated wheat plants at 216 dpi with *Puccinia striiformis* f. sp. *tritici* (*Pst*). The chlorosis of leaves, as an indicator for *Pst* sporulation capacity, in pEDV6:PSTha5a23-inoculated wheat plants was greater compared to that in control wheat plants.

Fig. S7. Fungal biomass measurements using qRT-PCR analysis of total DNA extracted from the pEDV6:eGFP- (control) and pEDV6:PSTha5a23-inoculated wheat

total wheat DNA was assessed using the *Pst* gene *PsEF1* and the wheat gene *TaEF1*. Values represent the means ± standard error of three independent assays. Differences were assessed using Student's t-tests, and asterisks indicate $P < 0.05$.

Fig. S8. Cytological observation of fungal growth in pEDV6:eGFP- (control) and pEDV6:PSTha5a23-inoculated wheat plants at 72 hpi with *Puccinia striiformis* f. sp. *tritici* (*Pst*). The fungal colony in pEDV6:PSTha5a23-inoculated wheat plants as greater compared to that in control wheat plants. Bar = 20 μm.

Fig. S9. The agarose gel electrophoresis from RNA samples used in this study. U, urediniospores; GU, germinated urediniospores; 18h – 216h, wheat leaves infected with *Puccinia striiformis* f. sp. *tritici* (*Pst*) at 18 – 216 hpi; B, barberry (*Berberis* spp.) leaves infected with *Pst* at 11 dpi. M, DM2000 DNA marker (CWBIO, Beijing, China).

Fig. S10. The agarose gel electrophoresis from *PSTha5a23* and *PsEF1* amplifications in several *Puccinia striiformis* f. sp. *tritici* (*Pst*) infection stages with their primers for qRT-PCR. 120 h – 216 h, wheat leaves infected with *Pst* at 120 – 216 hpi; B, barberry (*Berberis* spp.); M, DM2000 DNA marker (CWBIO, Beijing, China).

Fig. S11. The melting curves of *PsEF1* (A) and *PSTha5a23* (B) primers in qRT-PCR.

Fig. S12. Standard curves of *PsEF1* (A) and *PSTha5a23* (B) generated from seven serial dilutions of cDNA samples.

Fig. S13. Standard curves generated for the absolute quantification of *Puccinia striiformis* f. sp. *tritici* (*Pst*) (A) and wheat (B). Threshold cycles (Ct) are plotted against the initial copy number of template DNA (10^3, 10^4, 10^5, 10^6, 10^7, 10^8, and 10^9). Genomic DNA of the wheat cv. Suwon 11 and the *Pst* isolate CYR32 were used to construct the standard curves.

Table S1 Primers used in this study.

This article has been accepted for publication and undergone full peer review but has not been through the copyediting, typesetting, pagination and proofreading process which may lead to differences between this version and the Version of Record. Please cite this article as an 'Accepted Article', doi: 10.1111/1462-2920.13610

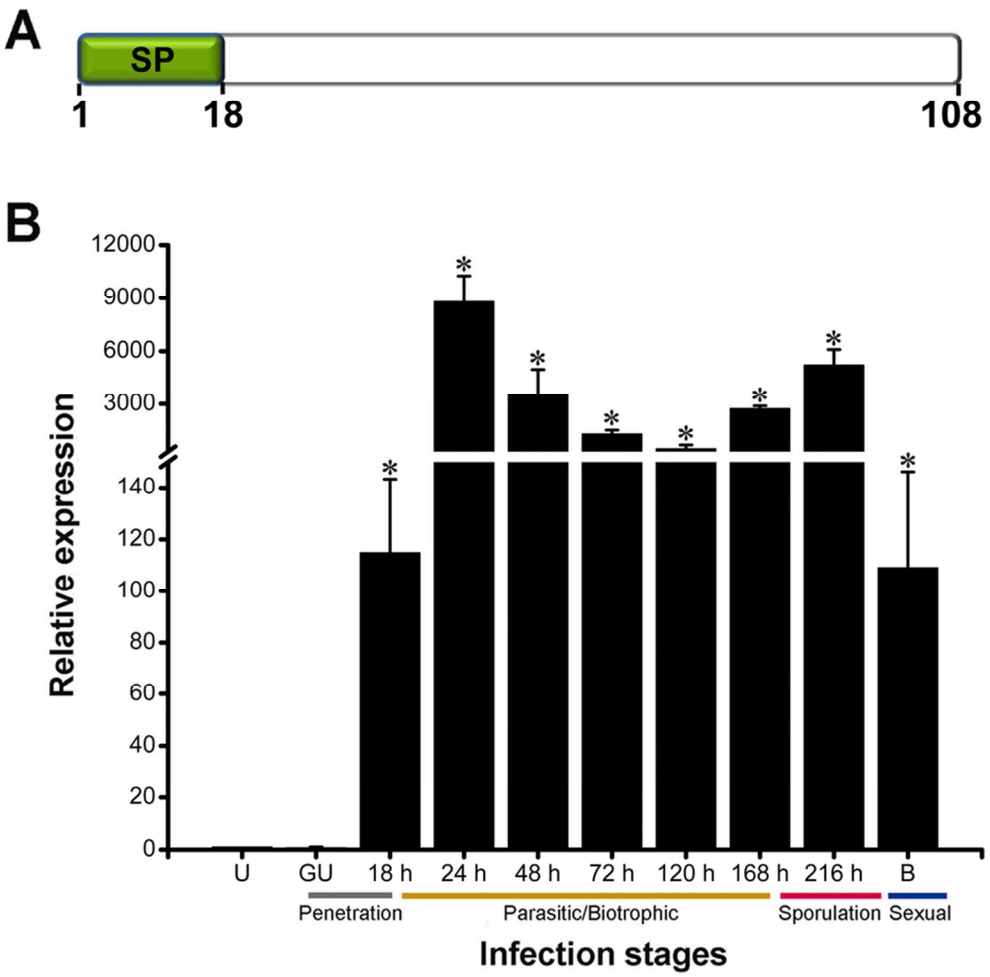

Fig. 1. The candidate effector PSTha5a23 is highly induced in planta. (A) Features of the primary structures of PSTha5a23. SP, signal peptide. (B) Transcription profiles of PSTha5a23 at different Puccinia striiformis f. sp. tritici (Pst) infection stages determined by qRT-PCR. Pst development in wheat can be divided into three major stages: penetration stage (gray), parasitic/biotrophic stage (yellow), and sporulation stage (red). Sexual reproduction on the alternate host Berberis is marked in blue. U, urediniospores; GU, germinated urediniospores; 18 h – 216 h, wheat leaves infected with Pst at 18 – 216 hpi; B, barberry (Berberis spp.) leaves infected with Pst at 11 dpi. Relative transcript levels were calculated using the Pfaffl analysis method, and values are expressed relative to an endogenous Pst reference gene EF1. The results represent the means ± standard errors of three biological replicates. Asterisks indicate a significant difference ($P < 0.05$) relative to the urediniospore sample determined using Student's t-test.

86x84mm (300 x 300 DPI)

This article has been accepted for publication and undergone full peer review but has not been through the copyediting, typesetting, pagination and proofreading process which may lead to differences between this version and the Version of Record. Please cite this article as an 'Accepted Article', doi: 10.1111/1462-2920.13610

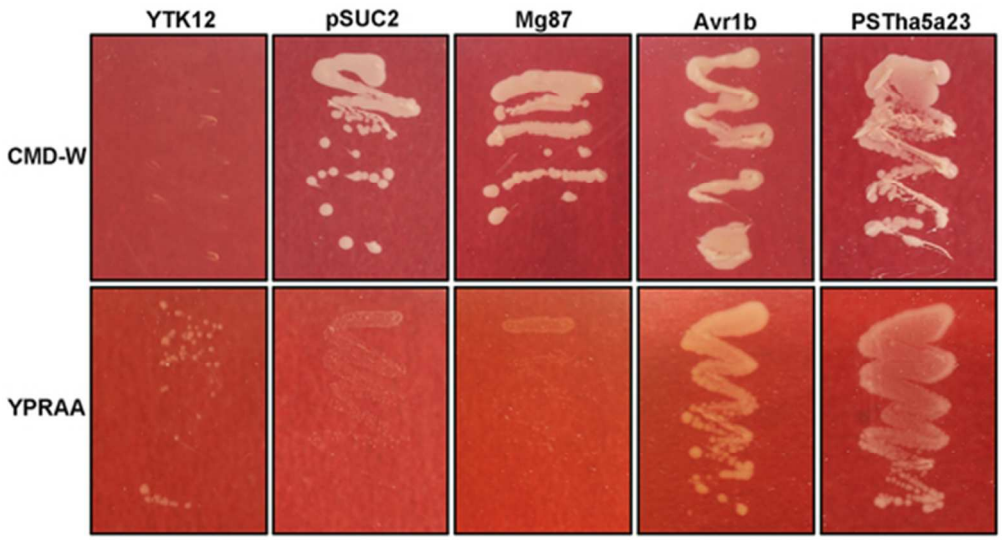

Fig. 2. Functional validation of the putative N-terminal signal peptide of PSTha5a23 using the yeast invertase secretion assay. The sequence of the putative PSTha5a23 signal peptide (Fig. 1 A) was fused in-frame to the invertase sequence in the pSUC2 vector and then transformed into yeast strain YTK12. The untransformed YTK12 strain, empty pSUC2 vector, and the first 25 aa of non-secreted Mg87 protein from Magnaporthe oryzae were used as negative controls, and the oomycete effector Avr1b was used as a positive control. Only the yeast strains that are able to secrete invertase can grow on both CMD-W and YPRAA media.

47x25mm (300 x 300 DPI)

This article has been accepted for publication and undergone full peer review but has not been through the copyediting, typesetting, pagination and proofreading process which may lead to differences between this version and the Version of Record. Please cite this article as an 'Accepted Article', doi: 10.1111/1462-2920.13610

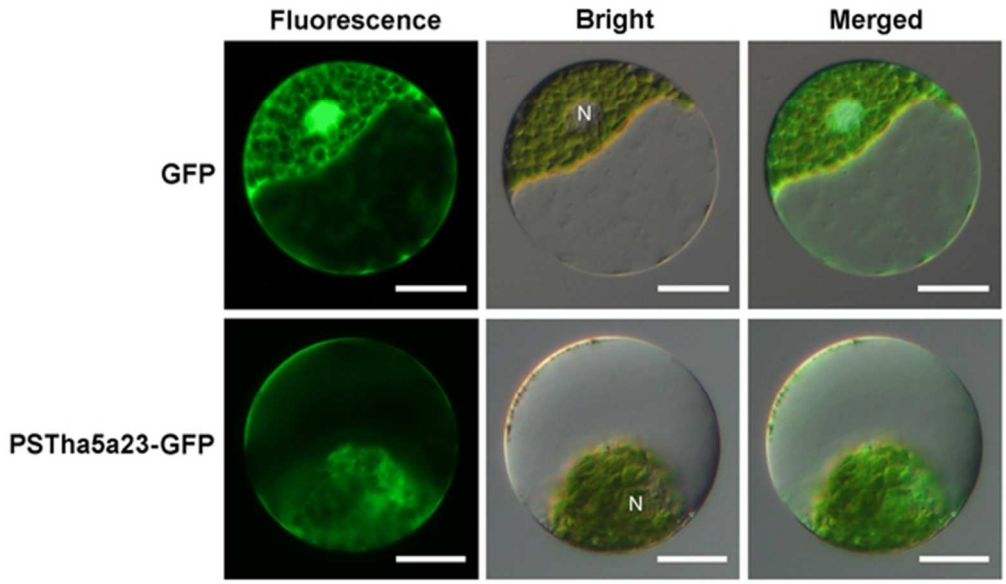

Fig. 3. Subcellular localization of PSTha5a23 in wheat protoplasts. GFP and PSTha5a23-GFP fusion proteins were expressed in wheat protoplasts following PEG-mediated transformation. N, nucleus. Bar = 20 μm.

51x30mm (300 x 300 DPI)

This article has been accepted for publication and undergone full peer review but has not been through the copyediting, typesetting, pagination and proofreading process which may lead to differences between this version and the Version of Record. Please cite this article as an 'Accepted Article', doi: 10.1111/1462-2920.13610

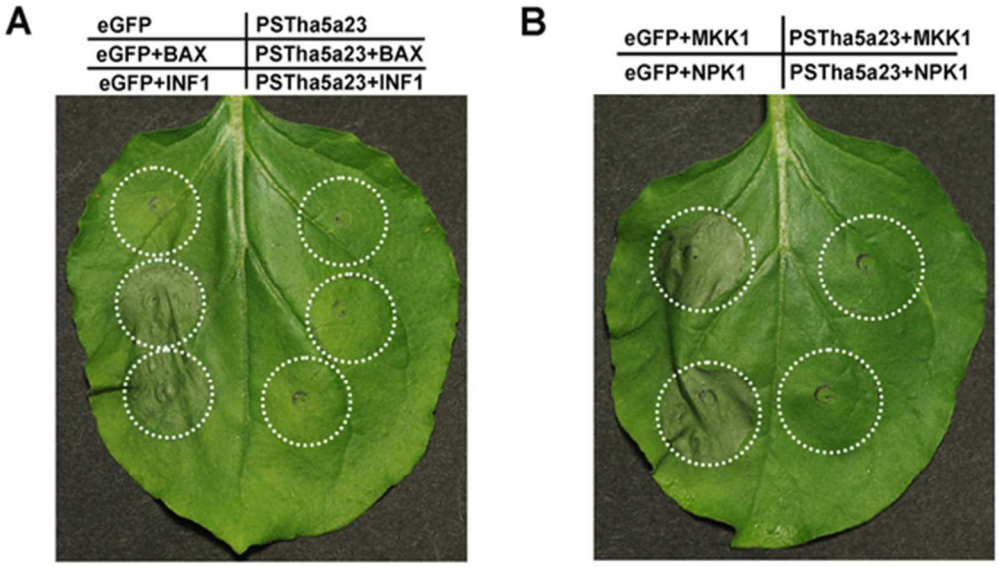

Fig. 4. Overexpression of PSTha5a23 in Nicotiana benthamiana suppressed programmed cell death triggered by BAX, PAMP-INF1 (A), and two resistance-related MAPKs (MKK1 and NPK1) (B). N. benthamiana leaves were infiltrated with Agrobacterium tumefaciens cells containing PVX carrying PSTha5a23 or a control gene (eGFP), either alone or followed after 24 h by A. tumefaciens cells carrying PVX:BAX/INF1/MKK1/NPK1.

50x28mm (300 x 300 DPI)

This article has been accepted for publication and undergone full peer review but has not been through the copyediting, typesetting, pagination and proofreading process which may lead to differences between this version and the Version of Record. Please cite this article as an 'Accepted Article', doi: 10.1111/1462-2920.13610

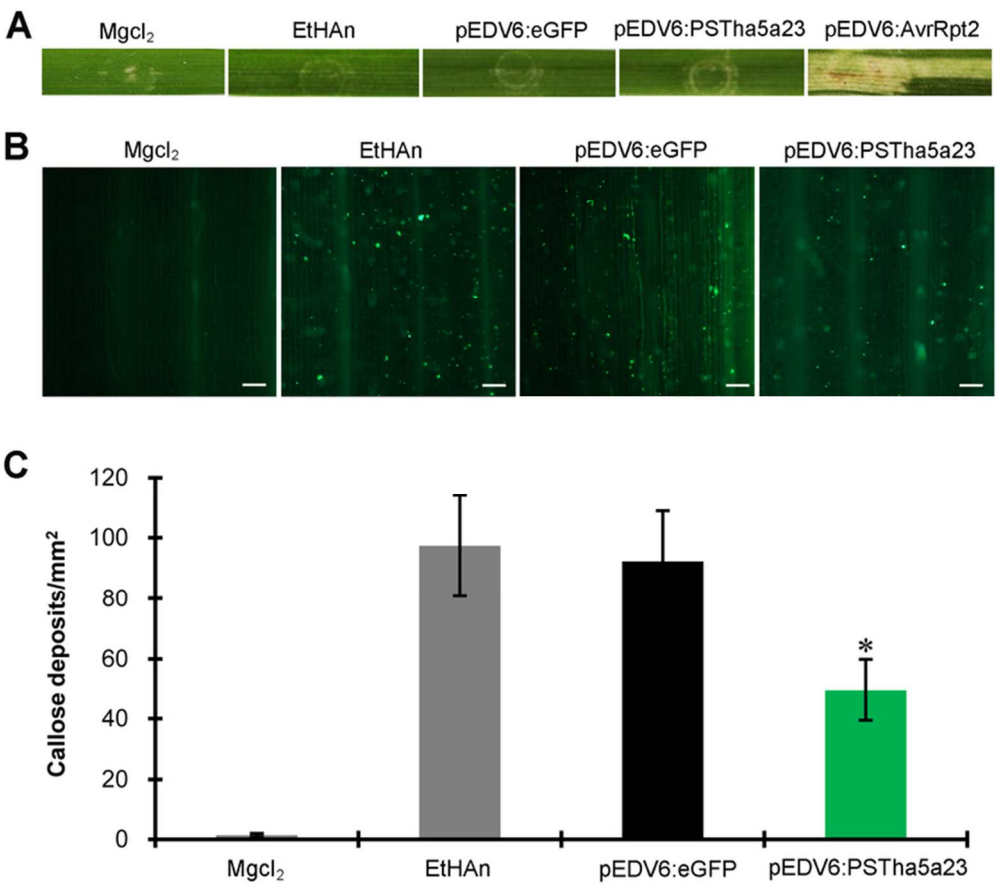

Fig. 5. Overexpression of PSTha5a23 in wheat (AvS) suppressed PTI-associated callose deposition. (A) The phenotype of wheat leaves inoculated with MgCl2 buffer, EtHAn, pEDV6:eGFP, pEDV6:PSTha5a23, and pEDV6:AvrRpt2 at 72 hpi. (B) The wheat leaves inoculated with MgCl2 buffer, EtHAn, pEDV6:eGFP, or pEDV6:PSTha5a23 were examined for callose deposition by epifluorescence microscopy after aniline blue staining. Bars = 100 µm. (C) Average number of callose deposits/mm2 in wheat leaves inoculated with MgCl2 buffer, EtHAn, pEDV6:eGFP, or pEDV6:PSTha5a23. Values represent the means ± standard error of three independent samples. Asterisks indicate a significant difference ($P < 0.05$) relative to the pEDV6:eGFP sample according to Student's t-test.

70x62mm (300 x 300 DPI)

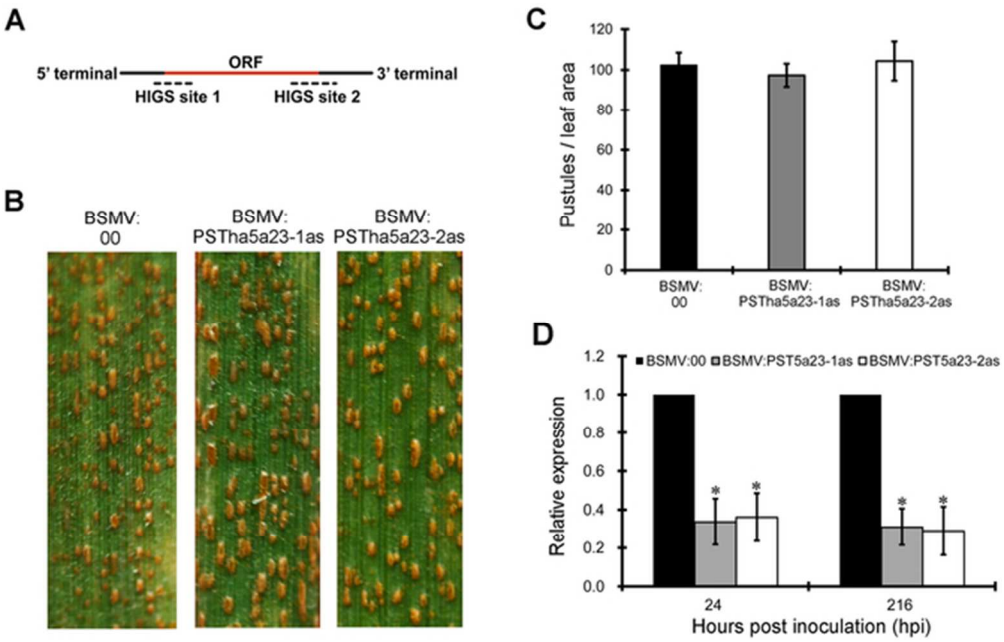

Fig. 6. Functional assessment of PSTha5a23 in Puccinia striiformis f. sp. tritici (Pst) pathogenicity determined by BSMV-mediated HIGS. (A) Two specific sequence regions for HIGS of PSTha5a23. (B) Phenotypes of the fourth leaves of BSMV:00- (control), BSMV:PSTha5a23-1as-, and BSMV:PSTha5a23-2as-inoculated wheat plants 14 dpi with Pst. (C) Quantification of the uredinial density in the BSMV:00-, BSMV:PSTha5a23-1as-, and BSMV:PSTha5a23-2as-inoculated wheat plants 14 dpi with Pst. Values represent the means ± standard error of three independent assays. (D) Relative transcript levels of PSTha5a23 in the BSMV:00-, BSMV:PSTha5a23-1as-, and BSMV:PSTha5a23-2as-inoculated wheat plants 24 and 216 hpi with Pst. Values are expressed relative to the endogenous Pst reference gene EF1, with the empty vector (BSMV:00) set at 1. Values represent the means ± standard error of three independent samples. Differences were assessed using Student's t-tests, and asterisks indicate $P < 0.05$.

56x36mm (300 x 300 DPI)

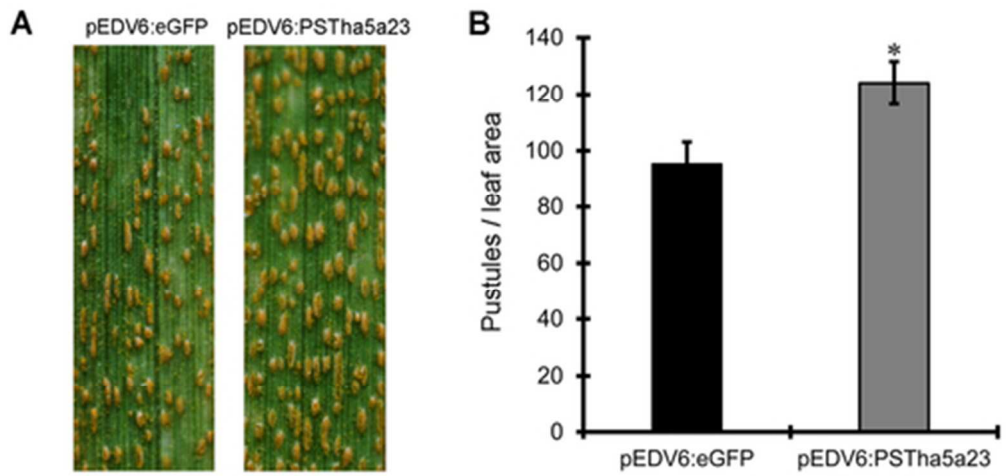

Fig. 7. Functional assessment of PSTha5a23 in Puccinia striiformis f. sp. tritici (Pst) pathogenicity determined by T3SS-mediated overexpression in wheat (Suwon 11). (A) Disease phenotypes of pEDV6:eGFP- (control) and pEDV6:PSTha5a23-inoculated wheat plants 14 dpi with Pst. (B) Quantification of uredinial density in pEDV6:eGFP- and pEDV6:PSTha5a23-inoculated wheat plants 14 dpi with Pst. Values represent the means ± standard error of three independent assays. Differences were assessed using Student's t-tests, and asterisks indicate $P < 0.05$.

42x20mm (300 x 300 DPI)

This article has been accepted for publication and undergone full peer review but has not been through the copyediting, typesetting, pagination and proofreading process which may lead to differences between this version and the Version of Record. Please cite this article as an 'Accepted Article', doi: 10.1111/1462-2920.13610